AIAA 81-4107

Optimization of Truss Structures Having Local and System Geometric Imperfections

Aviv Rosen*
Technion—Israel Institute of Technology, Haifa, Israel
and
Lucien A. Schmit Jr.†
University of California, Los Angeles, Calif.

A method to optimize truss structures, having both local and system geometric imperfections, is presented. The design is subjected to side, stress, displacement, local buckling, and system buckling constraints. During the optimization process an approximate analysis was used in order to obtain an efficient and practical method. Numerical optimization results for a 17-bar truss structure are presented. It is shown that small imperfections affect the optimum design considerably and lead to optimum designs with material distributions distinctly different from those obtained ignoring imperfections. It is also shown that previously suggested simple correction techniques for coping with the presence of imperfections do not yield optimum designs and, therefore, a systematic approach, such as presented herein, is needed.

I. Introduction

IT is well known that optimization of structures causes different modes of failure to coincide. As pointed out by Koiter and Skaloud,[1] simultaneous failure might give rise to severe imperfection sensitivity which can destroy this optimum. This problem has also been raised by others, for example, Thompson et al.[2-5] The reaction of the designers to this problem has been either hesitation to use optimization, or avoidance of the problem through the use of safety factors.[6] It is likely that the correct answer to this problem should be based on including the influence of imperfections in the analysis, while optimizing the structure.

There are relatively few previously published studies in which structures are optimized, taking into account the presence of imperfections. The influence of local geometric imperfections on the optimum design of lattice columns was discussed by Thompson and Hunt[5] and Crawford and Hedgepeth.[7] The latter investigators also studied the influence of local imperfections on the optimum design of truss-core sandwich panels. The structural analysis used in these investigations was a simplified one that neglected many important effects. Furthermore, none of these previous investigations considered the important influence of system imperfections on the structures that were examined.

In a recent paper[8] the present authors presented a method of analysis for predicting the behavior of truss structures taking both member and system geometric imperfections into account. Since imperfect truss structures exhibit a highly nonlinear behavior this nonlinear analysis was very expensive and time consuming. Therefore, in a later paper[9] a design oriented approximate analysis method for efficiently estimating the change in the behavior response of geometrically imperfect truss structures that undergo changes in the elements' cross sections was presented. This approximate analysis, which is faster and cheaper than the more accurate and complete iterative nonlinear analysis method,[8] provides an adequate foundation on which to build an optimization capability for imperfect truss structures.

The present paper presents optimization of truss structures which suffer from both local and system geometric imperfections and the design is subjected to side, displacement, stress, local buckling, and system buckling constraints.

II. Theory

A. Background Results

A truss structure is composed of M truss elements. Figure 1 shows the truss element i spanning between its boundary points P and Q. The length of the unloaded element is L_i, and its uniform cross-sectional area is A_i. The coordinates X, Y, and Z are fixed in space while x is a local coordinate connecting the boundary points P and Q. The geometric initial imperfection of the element is given by the following initial transverse deflection:

$$w_{0i} = b_{0i} \sin(\pi x / L_i) \tag{1}$$

where b_{0i} is the amplitude of the local initial imperfection.

The element is acted upon by an end force F_{ik}, associated with load condition k. The force F_{ik} acting on the imperfect truss element causes both pure tension or compression and bending. As a result, at the midspan of the element ($x = L_i/2$), two extreme stresses, a maximum and a minimum, appear at

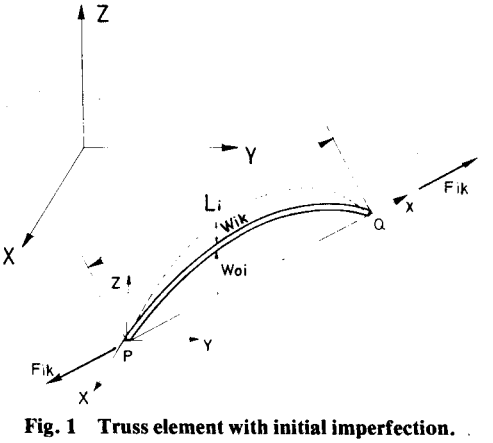

Fig. 1 Truss element with initial imperfection.

Received Oct. 1, 1979; revision received Dec. 2, 1980.

*Senior Lecturer, Department of Aeronautical Engineering. Member AIAA.

†Professor of Engineering and Applied Science, Mechanics and Structures Department. Associate Fellow AIAA.

the two extreme points of the cross section, measured with relation to the neutral axis of bending. These two stresses are given by [Eq. (15) of Ref. 8]:

$$(\sigma_{ik})_{\max,\min} = \frac{F_{ik}}{A_i}\left[1 \pm \frac{b_{0i} y_{ci}}{r_i^2}\,\frac{d_{ik}}{1+d_{ik}}\right] \tag{2}$$

where y_{ci} in Eq. (2) is the distance from the extreme fiber to the neutral axis. In the case of a cross section that is not symmetric there are two extreme fiber distances to consider: one is in tension and the other is compressed by bending. Since the direction of the initial imperfection must be regarded as random, it is reasonable to take y_{ci} as the larger of the two extreme fiber distances. The symbol r_i in Eq. (2) represents the radius of gyration given by

$$r_i^2 = I_i / A_i \tag{3a}$$

where I_i is the smaller of the two principal-axis moments of inertia. The notation d_{ik} that appears in Eq. (2) is defined by

$$d_{ik} = P_{Ei} / F_{ik} \tag{3b}$$

while P_{Ei}, the Euler buckling load of the element, is given by

$$P_{Ei} = \pi^2 E_i I_i / L_i^2 \tag{3c}$$

where E_i is Young's modulus of the element.

In order to obtain the nodal displacements and the member forces, the equilibrium state must be determined. This is done by assembling the stiffness matrix of the entire structure. In order to assemble this matrix the stiffness matrix for each element must be generated. In the case of imperfect truss elements the stiffness of each element depends on the force in the element [see Eqs. (17) and (18) of Ref. 8] and in general this force can only be found by solving the entire system of equilibrium equations. It is thus apparent that the structural analysis problem is nonlinear. Furthermore, in order to include the influence of system imperfections, geometric contributions to the stiffness matrices (assuming small rotations of the elements) are included in the formulation. This introduces an additional nonlinear feature into the structural analysis.

As explained in Ref. 8, the nonlinear set of equations is solved iteratively for the displacements. After convergence the nodal displacements and the member forces are known. This nonlinear analysis is very expensive and time consuming and therefore inappropriate for optimization purposes where a large number of analyses is required. Therefore, a more efficient and faster approximate analysis was developed.[9] This approximate analysis is based on a complete nonlinear accurate analysis of a certain design, called the base design, and it predicts the change in the behavior of the structure as a result of varying the elements' cross sections compared to the base design.

The approximate expression for the displacement of node j in the direction ℓ (X, Y, or Z direction) under load conditions k is given by [Eq. (4) of Ref. 9]

$$u_{j\ell k} = (u_{j\ell k})_0 + \sum_{i=1}^{M} \left(\frac{\partial u_{j\ell k}}{\partial \beta_{ik}}\right)_0 [\beta_{ik} - (\beta_{ik})_0] \tag{4}$$

The subscript zero indicates quantities evaluated at the base design point. Calculation of displacement component derivatives with respect to the β_{ik} was discussed in Ref. 9 and it will not be repeated here. β_{ik} is given by [Eq. (3) of Ref. 9]

$$\beta_{ik} = \left[1 + \gamma_{ik}\frac{1+2d_{ik}}{(1+d_{ik})^2}\right] \Big/ A_i \tag{5a}$$

while

$$\gamma_{ik} = (b_{0i}^2 / 4r_i^2)\, d_{ik} \tag{5b}$$

The results given in Ref. 9 indicate that this approximation gives good results even in regions where fairly strong nonlinearity exists.

It is important to note[9] that during the approximate analyses, while changing the cross sections, changes in the member forces can be neglected, so that

$$F_{ik} = (F_{ik})_0 \tag{6}$$

In addition to the displacement response analysis, Ref. 8 also includes an analysis for predicting the buckling load factor of imperfect truss structures. The buckling analysis leads to a nonlinear eigenvalue problem because the stiffness matrix is a function of the forces in the truss elements. Therefore, this eigenvalue problem is also solved iteratively. It is assumed in the buckling load factor calculations that the force distribution in the structure at the onset of buckling is proportional to the force distribution obtained from the last complete nonlinear displacement behavior analysis.

An efficient approximate scheme for predicting the buckling load factor after changes in the member cross sections was also developed.[9] Numerical examples presented indicate that this approximate analysis gives good quality results. According to this approximate theory the buckling load factor for mode ℓ under load condition k is given by [Eq. (15) of Ref. 9]

$$\lambda_{\ell k} = \lambda_{\ell k 0} + \sum_{i=1}^{M} \left\{ \left(\frac{\partial \lambda_{\ell k}}{\partial \tilde{A}_{ik}}\right)_{\lambda \ell k 0} [(\tilde{A}_{ik})_{\lambda \ell k} - (\tilde{A}_{ik})_{\lambda \ell k 0}] \right\} \tag{7a}$$

where

$$\tilde{A}_{ik} = 1/\beta_{ik} \tag{7b}$$

and $\lambda_{\ell k 0}$ represents the buckling factor for the mode ℓ under load condition k, at the base design (before any changes in the cross sections are made). The notation $(\partial \lambda_{\ell k}/\tilde{A}_{ik})_{\lambda \ell k 0}$ denotes the first derivative of the buckling load factor with respect to the equivalent cross-sectional area $\tilde{A}_{ik}$ (for details see Ref. 9) evaluated when the load factor equals $\lambda_{\ell k 0}$ and the symbols $(\tilde{A}_{ik})_{\lambda \ell k}$ and $(\tilde{A}_{ik})_{\lambda \ell k 0}$ represent values of $(\tilde{A}_{ik})$ when the load factor is $\lambda_{\ell k}$ and $\lambda_{\ell k 0}$, respectively. The fact that $(\tilde{A}_{ik})_{\lambda \ell k}$ is a function of $\lambda_{\ell k}$ implies that Eq. (7a) itself is nonlinear and, therefore, it is solved in an iterative manner.

B. Design Variables

It is assumed that there are N design variables associated with the design of a particular truss structure. In this study only changes of the member cross sections are treated and the configuration is held fixed. The design variables are denoted by x_α where α takes on integer values between 1 and N. It should be recognized that x_α is not necessarily associated with element α because, generally speaking, each element can have more than one design variable, or on the other hand, several elements can have one common design variable. It is assumed that the material properties, the element lengths, and the imperfection shapes are independent of the design variables. The quantities that are functions of the design variables are

$$A_i,\ I_i,\ y_{ci} \tag{8a}$$

and as a result of Eq. (8a) it follows that the quantities

$$P_{Ei},\ d_{ik},\ \beta_{ik},\ \tilde{A}_{ik} \tag{8b}$$

become functions of the design variables.

The detailed explicit dependence of the quantities appearing in Eqs. (8a) and (8b) on the independent design variables depends upon the specific cross-sectional shapes and the design variables selected.

It will become apparent in the sequel that derivatives of the terms appearing in Eq. (8b) with respect to the independent design variables are needed. Since the quantities in Eq. (8b) depend on the cross-sectional properties in Eq. (8a), a few simplifications can be made.

According to Eq. (3c) (remembering that E_i and L_i are not functions of the design variables)

$$\frac{\partial P_{Ei}}{\partial x_\alpha} = \frac{\pi^2 E_i}{L_i^2} \frac{\partial I_i}{\partial x_\alpha} \tag{9a}$$

$$\frac{\partial^2 P_{Ei}}{\partial x_\alpha \partial x_\beta} = \frac{\pi^2 E_i}{L_i^2} \frac{\partial^2 I_i}{\partial x_\alpha \partial x_\beta} \tag{9b}$$

In view of Eq. (3b) and assumption Eq. (6)

$$\frac{\partial d_{ik}}{\partial x_\alpha} = \frac{1}{F_{ik}} \frac{\partial P_{Ei}}{\partial x_\alpha} \tag{10a}$$

$$\frac{\partial^2 d_{ik}}{\partial x_\alpha \partial x_\beta} = \frac{1}{F_{ik}} \frac{\partial^2 P_{Ei}}{\partial x_\alpha \partial x_\beta} \tag{10b}$$

Furthermore, Eq. (5a) can be written as

$$\beta_{ik} = \frac{1}{A_i} + \eta_{ik} \frac{1+2d_{ik}}{(1+d_{ik})^2} \tag{11a}$$

where

$$\eta_{ik} = \frac{b_{0i}^2 E_i \pi^2}{4 L_i^2 F_{ik}} \tag{11b}$$

and under the present assumptions η_{ik} is not dependent on the design variables, therefore,

$$\frac{\partial \beta_{ik}}{\partial x_\alpha} = -\frac{\partial A_i / \partial x_\alpha}{A_i^2} + \eta_{ik} \frac{-2d_{ik}(\partial d_{ik}/\partial x_\alpha)}{(1+d_{ik})^3} \tag{12a}$$

$$\frac{\partial^2 \beta_{ik}}{\partial x_\alpha \partial x_\beta} = \frac{2 \dfrac{\partial A_i}{\partial x_\alpha} \dfrac{\partial A_i}{\partial x_\beta} - A_i \dfrac{\partial^2 A_i}{\partial x_\alpha \partial x_\beta}}{A_i^3}$$

$$+ 2\eta_{ik} \frac{\dfrac{\partial d_{ik}}{\partial x_\alpha} \dfrac{\partial d_{ik}}{\partial x_\beta} (2d_{ik}-1) - \dfrac{\partial^2 d_{ik}}{\partial x_\alpha \partial x_\beta} d_{ik}(1+d_{ik})}{(1+d_{ik})^4} \tag{12b}$$

Also using Eq. (7a) it follows that

$$\frac{\partial \tilde{A}_{ik}}{\partial x_\alpha} = -\frac{\partial \beta_{ik}/\partial x_\alpha}{\beta_{ik}^2} \tag{13a}$$

$$\frac{\partial^2 \tilde{A}_{ik}}{\partial x_\alpha \partial x_\beta} = \frac{2 \dfrac{\partial \beta_{ik}}{\partial x_\alpha} \dfrac{\partial \beta_{ik}}{\partial x_\beta} - \beta_{ik} \dfrac{\partial^2 \beta_{ik}}{\partial x_\alpha \partial x_\beta}}{\beta_{ik}^3} \tag{13b}$$

Examination of Eqs. (9-13) reveals that the only additional sensitivity information needed at this juncture is the first and second derivatives of A_i and I_i with respect to the design variables. However, it should be noted that the derivatives of y_{ci} with respect to the design variables will be required in order to evaluate the sensitivity of the stress constraints.

In deriving the constraint derivatives it is assumed that the constraints behave according to the approximate expressions. The constraints are defined so that they are positive in the feasible region. The constraints and their derivatives are given in detail so that it is possible to recognize the nonlinear complicated nature of the expressions compared to previous cases[10] where perfect truss structures were optimized.

C. Side Constraints

Side constraints refer to lower and/or upper limits placed on intermediate variables or design variables. In the class of problems addressed here, side constraints could be placed on the cross-sectional properties or on the design variables x_α themselves. In the current formulation lower and upper constraints on the cross-sectional areas are introduced.

Upper Limit Constraints

If the maximum allowable cross-sectional area of element i is denoted by $A_{i,\text{upper}}$ then the appropriate constraint is

$$G = 1 - A_i / A_{i,\text{ upper}} \tag{14}$$

This means that in the feasible region the value of the constraint is positive. The first and second derivatives of the constraint, with respect to the design variables, are

$$\frac{\partial G}{\partial x_\alpha} = -\frac{1}{A_{i,\text{ upper}}} \frac{\partial A_i}{\partial x_\alpha} \tag{15a}$$

$$\frac{\partial^2 G}{\partial x_\alpha \partial x_\beta} = -\frac{1}{A_{i,\text{ upper}}} \frac{\partial^2 A_i}{\partial x_\alpha \partial x_\beta} \tag{15b}$$

Lower Limit Constraints

If the minimum allowable cross-sectional area of element i is denoted by $A_{i,\text{ lower}}$ then the appropriate constraint is

$$G = 1 + A_i / A_{i,\text{ lower}} \tag{16}$$

The derivatives of the constraint are

$$\frac{\partial G}{\partial x_\alpha} = \frac{1}{A_{i,\text{ lower}}} \frac{\partial A_i}{\partial x_\alpha} \tag{17a}$$

$$\frac{\partial^2 G}{\partial x_\alpha \partial x_\beta} = \frac{1}{A_{i,\text{ lower}}} \frac{\partial^2 A_i}{\partial x_\alpha \partial x_\beta} \tag{17b}$$

D. Stress Constraints

From Eqs. (2) and (3) it follows that

$$\sigma_{ik,\text{ max,min}} = \frac{F_{ik}}{A_i} \pm \xi_i \frac{y_{ci}}{1+d_{ik}} \tag{18a}$$

where

$$\xi_i = (b_{0i} E_i \pi^2) / L_i^2 \tag{18b}$$

It is clear that under the present assumptions ξ_i is constant and does not depend on the design variables. For each case the two values generated by Eq. (18a), one with the minus sign and the other with the plus sign, refer to the maximum and

minimum values of the stress, which is decided simply by comparing them. The derivatives of the stresses with respect to the design variables are obtained by differentiating Eq. (18a) and using Eq. (6). This yields

$$\frac{\partial \sigma_{ik,\,\max,\min}}{\partial x_\alpha} = -\frac{F_{ik}}{A_i^2}\frac{\partial A_i}{\partial x_\alpha} \pm \xi_i \frac{\dfrac{\partial y_{ci}}{\partial x_\alpha}(1+d_{ik}) - y_{ci}\dfrac{\partial d_{ik}}{\partial x_\alpha}}{(1+d_{ik})^2} \tag{19a}$$

$$\frac{\partial^2 \sigma_{ik,\,\max,\min}}{\partial x_\alpha \partial x_\beta} = \frac{2\dfrac{\partial A_i}{\partial x_\alpha}\dfrac{\partial A_i}{\partial x_\beta} - A_i\dfrac{\partial^2 A_i}{\partial x_\alpha \partial x_\beta}}{A_i^3}$$
$$\pm \xi_i \left\{ \left[\frac{\partial^2 y_{ci}}{\partial x_\alpha \partial x_\beta}(1+d_{ik}) - \frac{\partial y_{ci}}{\partial x_\alpha}\frac{\partial d_{ik}}{\partial x_\beta} - \frac{\partial y_{ci}}{\partial x_\beta}\frac{\partial d_{ik}}{\partial x_\alpha} - y_{ci}\frac{\partial^2 d_{ik}}{\partial x_\alpha \partial x_\beta} \right](1+d_{ik}) + 2\frac{\partial d_{ik}}{\partial x_\alpha}\frac{\partial d_{ik}}{\partial x_\beta} y_{ci} \right\} \Big/ (1+d_{ik})^3 \tag{19b}$$

The stresses in the element i are bounded by upper and lower limits given by $\sigma_{i,\,\text{upper}}$ and $\sigma_{i,\,\text{lower}}$, respectively. Let the normalizing parameter $\bar{\sigma}_i$ be defined as

$$\bar{\sigma}_i = (\sigma_{i,\,\text{upper}} - \sigma_{i,\,\text{lower}})/2 \tag{20}$$

Upper Limit Constraints

In this case the constraint for element i under load condition k is given by

$$G = (\sigma_{i,\,\text{upper}} - \sigma_{ik,\,\max})/\bar{\sigma}_i \tag{21}$$

Clearly the derivatives of the constraint are

$$\frac{\partial G}{\partial x_\alpha} = -\frac{1}{\bar{\sigma}_i}\frac{\partial \sigma_{ik,\,\max}}{\partial x_\alpha} \tag{22a}$$

$$\frac{\partial^2 G}{\partial x_\alpha \partial x_\beta} = -\frac{1}{\bar{\sigma}_i}\frac{\partial^2 \sigma_{ik,\,\max}}{\partial x_\alpha \partial x_\beta} \tag{22b}$$

The derivatives of the stresses are given by Eqs. (19).

Lower Limit Constraints

In this case the constraint for element i under load condition k is given by

$$G = (\sigma_{ik,\,\min} - \sigma_{i,\,\text{lower}})/\bar{\sigma}_i \tag{23}$$

The derivatives of the constraint are

$$\frac{\partial G}{\partial x_\alpha} = \frac{1}{\bar{\sigma}_i}\frac{\partial \sigma_{ik,\,\min}}{\partial x_\alpha} \tag{24a}$$

$$\frac{\partial^2 G}{\partial x_\alpha \partial x_\beta} = \frac{1}{\bar{\sigma}_i}\frac{\partial^2 \sigma_{ik,\,\min}}{\partial x_\alpha \partial x_\beta} \tag{24b}$$

The derivatives of the stresses are given by Eqs. (19).

E. Displacement Constraints

The displacement of node j in the direction ℓ can be bounded by upper and lower limits given by $u_{j\ell,\,\text{upper}}$ and $u_{j\ell,\,\text{lower}}$, respectively. Let the normalizing parameter $\bar{u}_{j\ell}$ be defined as

$$\bar{u}_{j\ell} = (u_{j\ell,\,\text{upper}} - u_{j\ell,\,\text{lower}})/2 \tag{25}$$

The displacement of node j in the direction ℓ under load condition k is given by Eq. (4). Therefore, the derivatives of the displacement with respect to the design variables are

$$\frac{\partial u_{j\ell k}}{\partial x_\alpha} = \sum_{i=1}^{M}\left(\frac{\partial u_{j\ell k}}{\partial \beta_{ik}}\right)_0 \frac{\partial \beta_{ik}}{\partial x_\alpha} \tag{26a}$$

$$\frac{\partial^2 u_{j\ell k}}{\partial x_\alpha \partial x_\beta} = \sum_{i=1}^{M}\left(\frac{\partial u_{j\ell k}}{\partial \beta_{ik}}\right)_0 \frac{\partial^2 \beta_{ik}}{\partial x_\alpha \partial x_\beta} \tag{26b}$$

Upper Limit Displacement Constraints

The upper limit displacement constraints are given by

$$G = (u_{j\ell,\,\text{upper}} - u_{j\ell k})/\bar{u}_{j\ell} \tag{27}$$

The derivatives of the constraint are

$$\frac{\partial G}{\partial x_\alpha} = -\frac{1}{\bar{u}_{j\ell}}\frac{\partial u_{j\ell k}}{\partial x_\alpha} \tag{28a}$$

$$\frac{\partial^2 G}{\partial x_\alpha \partial x_\beta} = -\frac{1}{\bar{u}_{j\ell}}\frac{\partial^2 u_{j\ell k}}{\partial x_\alpha \partial x_\beta} \tag{28b}$$

The derivatives of the displacements in Eqs. (28) are given by Eqs. (26).

Lower Limit Displacement Constraints

The lower limit displacement constraints are given by

$$G = (u_{j\ell k} - u_{j\ell,\,\text{lower}})/\bar{u}_{j\ell} \tag{29}$$

The derivatives of the constraint are

$$\frac{\partial G}{\partial x_\alpha} = \frac{1}{\bar{u}_{j\ell}}\frac{\partial u_{j\ell k}}{\partial x_\alpha} \tag{30a}$$

$$\frac{\partial^2 G}{\partial x_\alpha \partial x_\beta} = \frac{1}{\bar{u}_{j\ell}}\frac{\partial^2 u_{j\ell k}}{\partial x_\alpha \partial x_\beta} \tag{30b}$$

The derivatives of the displacements in Eqs. (30) are also given by Eqs. (26).

F. Local Buckling Constraints

The member buckling constraint is formulated so that the compressive force in member i under load condition k does not exceed some specified fraction of the member buckling load. For element i under load condition k this constraint has the following form:

$$G = 1.0 + \frac{F_{ik}}{s_{1i}P_{Ei}} = 1.0 + \frac{1}{s_{1i}d_{ik}} \tag{31}$$

where s_{1i} is a factor that is assigned a value between zero and one. The terms $s_{1i}P_{Ei}$ in Eq. (31) then represent a compressive force level smaller than the buckling load P_{Ei}, which is not exceeded.

The derivatives of the local buckling constraint are

$$\frac{\partial G}{\partial x_\alpha} = -\frac{1}{s_{1i}}\frac{\partial d_{ik}/\partial x_\alpha}{d_{ik}^2} \tag{32a}$$

$$\frac{\partial^2 G}{\partial x_\alpha \partial x_\beta} = -\frac{1}{s_{1i}}\frac{\dfrac{\partial^2 d_{ik}}{\partial x_\alpha \partial x_\beta}d_{ik} - 2\dfrac{\partial d_{ik}}{\partial x_\alpha}\dfrac{\partial d_{ik}}{\partial x_\beta}}{d_{ik}^3} \tag{32b}$$

G. System Buckling Constraints

The buckling load factor for mode ℓ under load condition k is given by Eqs. (7). The derivatives of this buckling load factor are

$$\frac{\partial \lambda_{\ell k}}{\partial x_\alpha} = \sum_{i=1}^{M} \left(\frac{\partial \lambda_{\ell k}}{\partial \tilde{A}_{ik}} \right)_{\lambda_{\ell k 0}} \left[\frac{\partial (\tilde{A}_{ik})_{\lambda_{\ell k}}}{\partial x_\alpha} \right] \tag{33a}$$

$$\frac{\partial^2 \lambda_{\ell k}}{\partial x_\alpha \partial x_\beta} = \sum_{i=1}^{M} \left(\frac{\partial \lambda_{\ell k}}{\partial \tilde{A}_{ik}} \right)_{\lambda_{\ell k 0}} \left[\frac{\partial^2 (\tilde{A}_{ik})_{\lambda_{\ell k}}}{\partial x_\alpha \partial x_\beta} \right] \tag{33b}$$

The constraint associated with the system buckling load factor has the following form:

$$G = c(\lambda_{\ell k} s_{2\ell} - 1) \tag{34a}$$

where

$$c = 1 \qquad \text{if } \lambda_{\ell k} > 0$$

$$c = -1 \qquad \text{if } \lambda_{\ell k} < 0 \tag{34b}$$

The $s_{2\ell}$ is a factor that is assigned a value between zero and one. As a result of the constraint embodied in Eqs. (34) the buckling load factor $\lambda_{\ell k}$ for mode ℓ under load condition k must equal or exceed $(1/s_{2\ell})$.

The derivatives of the constraint are

$$\frac{\partial G}{\partial x_\alpha} = c s_{2\ell} \frac{\partial \lambda_{\ell k}}{\partial x_\alpha} \tag{35a}$$

$$\frac{\partial^2 G}{\partial x_\alpha \partial x_\beta} = c s_{2\ell} \frac{\partial^2 \lambda_{\ell k}}{\partial x_\alpha \partial x_\beta} \tag{35b}$$

The derivatives of the buckling load factors in Eqs. (35) are given by Eqs. (33).

III. Optimization Procedure

The goal of the optimization process is to minimize the weight of the structure. The optimization procedure employed here basically follows the method used by Schmit and Miura.[10] At the outset the initial design is analyzed by the accurate complete method and an approximate representation of the structural behavior is constructed. This approximate representation is called a model and optimization of this model is executed. One should, therefore, note that, in what follows, "model" means an approximate representation of the structure near some base design and not, for example, a finite element model. The optimization is carried out by a sequence of unconstrained minimizations technique (SUMT) algorithm based on the Haftka-Starnes[11] extended interior penalty function formulation. At the end of the present optimization procedure a complete analysis of the optimized structure is executed. Using these analysis results, a new model is generated and the optimization procedure is then repeated. This chain of operations is continued until a predetermined convergence criterion is satisfied.

Using a quadratic extended interior penalty function[11] it should be remembered that this function has continuous first and second derivatives. The interior penalty function is extended into the infeasible domain and so it provides an automatic mechanism to recover from constraint violations that may arise due to the use of approximate analyses or the use of an infeasible initial design. In practice it was found that the process of returning from the infeasible to the feasible region is in many cases slow, expensive, and inefficient. Therefore, an option (which is used in the numerical example of this paper) to modify the design in order to get back into the feasible region has been provided in the computer code. While in ACCESS 1 scale up involved simple multiplication of all design variables by a constant greater than one, in the present program the design is modified by moving in the direction of the gradient to the violated constraint.

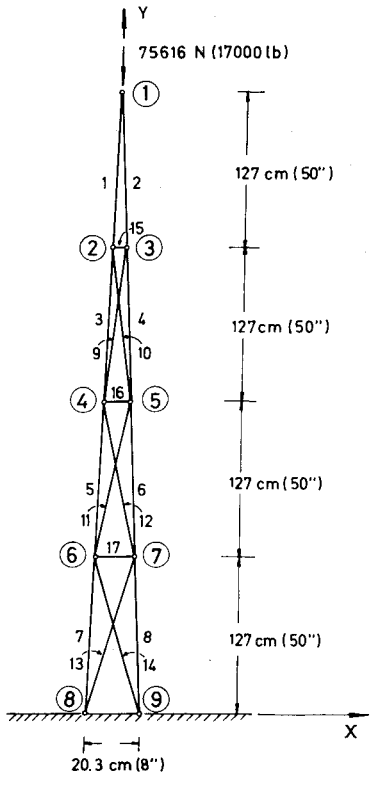

Fig. 2 17-bar truss structure.

The operator of the computer code has to determine three convergence criteria: convergence among one-dimensional minimizations in a certain response surface, convergence among response surfaces in a certain model, and convergence criterion among models. He also determines the maximum allowable number of response surfaces per model, and the maximum allowable number of one-dimensional minimizations per response surface.

IV. Numerical Example

As an example, optimization of a planar 17-bar truss structure including both local and system imperfections will be presented. The elements of the structure are considered uniform rectangular cross sections with a constant depth of 2.54 cm. The cross sectional properties A_i, I_i, and y_{ci} and their derivatives, as indicated in subsection B, easily are calculated.

Convergence criterion among models is that the relative change between the minimum weight of the last three models is less than 0.001. The convergence criterion in the one-dimensional minimization is even smaller and given as a maximum relative change of 0.0005. Only two response surfaces per model are allowed.

The geometry of this structure is presented in Fig. 2. The structure is loaded by a vertical compressive load of 75616 N as shown in the figure. The initial design, if not otherwise indicated, was as follows: The cross-sectional areas of elements 1-8 were taken as 19.35 cm^2 while the cross-sectional areas of the rest of the elements were 12.90 cm^2. The total weight of this initial design was 828.22 N. (Specific weight of the material is 2.768 g/cm^3.) Young's modulus of the material is 68940 MPa.

Four basic cases were considered: case I is a perfect structure. Case II is a structure with only local imperfections. The amplitude of the imperfections of elements 1-14 were taken equal to 0.254 cm while those of elements 15-17 were

taken as 0.0254 cm. Case III incorporated only system imperfections. The nodes of the structure were displaced slightly from their original position in the shape of the first mode of the buckling of the initial design. These displacements were performed only in the X direction (see Fig. 2) while the shift of node 1, which shows the largest shift among all nodes, was only 1.27 cm. Case IV at the same time incorporated the local imperfections of case II and the system imperfections of case III. One other case associated with the 17-bar structure will be described later in this section.

The design is subjected to side, stress, displacement, local buckling, and system buckling constraints. The side constraints include the restraint that any cross section is not allowed to be less than 0.645 cm^2. According to the stress constraints the absolute value of any stress, tension, or compression is not allowed to exceed 68.95 MPa. The displacement constraints incorporate the displacements of node number 1, where the displacement in the X direction is restricted not to exceed 2.54 cm, while the displacement in the Y direction is restricted to a maximum of 1.27 cm. The compressive force at any of the elements 1-14 is not allowed to exceed 90% of the Euler buckling load while a compressive force at elements 15-17 is not allowed to exceed 20% of the elements' Euler buckling load. The system buckling constraint implies that the compressive force that acts on the structure never exceeds 90% of the system buckling load.

In the design procedure a requirement for symmetry of the structure has been imposed, namely, that symmetric elements must be equal in size (the pairs of elements 1-2, 3-4, 5-6, 7-8, 9-10, 11-12, 13-14 are equal in size) so that only ten independent design variables exist.

Table 1 Weight information at the end of the optimization of each model of the 17-bar truss structure

Model	Case I	Case II	Case III	Case IV	Case V
0	828.2	828.2	828.2	828.2	1142.6
1	506.2	544.5	537.5	587.2	711.2
2	445.9	476.5	488.7	518.7	625.7
3	407.8	438.1	463.4	488.5	531.3[a]
					646.6
4	394.6	422.0	436.0[a]	476.0	565.6[a]
			448.6		631.7
5	380.1	418.3	435.1[a]	470.1[a]	576.6
			440.4	474.6	
6	376.2	412.2	429.3[a]	465.1[a]	580.1
			435.2	470.0	
7	374.5	410.2	428.7[a]	464.2[a]	574.3
			433.8	467.1	
8	373.2[a]	408.5[b]	427.5[a]	464.4[a]	572.4
	373.4	412.5	432.3	465.4	
9	373.1[a]	408.3[a]	427.2[a]	462.7[a]	570.7
	373.3	408.9	431.9	464.5	
10	372.5[a]	408.4[b]	431.4	462.6[a]	568.7
	373.1	412.9		463.5	
11	372.5[a]		431.3	461.9[a]	566.8
	372.9			462.9	
12	372.4[a]		431.1	462.6	564.9
	372.8				
13				462.5	563.7[a]
					565.0
14					564.4[a]
					565.2
15					564.5[a]
					578.0
16					564.2[a]
					564.8

N.B.: Results are in Newtons. [a] Infeasible design. [b] The nonlinear analysis does not converge. All the design variables are therefore increased by 1%.

A. Case I

The results for case I are presented in Tables 1 and 2. From Table 1 one can see that for models close to the optimum design there is a tendency, during the optimization process, to get slightly into the infeasible region. The weight of the structure after getting back into the feasible region is also given in Table 1. This tendency is the result of using an approximate representation of the behavior of the structure.

The cross-sectional areas of the different elements of the optimum design and the weight of total structure are given in Table 2. The active constraints are local buckling constraints that determine the sizes of elements 1-14. The sizes of elements 16 and 17 are determined by their stress constraints. It is interesting to note that element 15 is not determined by a particularly evident constraint. The reason for this is the fact that, even if the cross-sectional area of element 15 would have been reduced to 0.645 cm^2 which is the smaller allowable value according to the side constraint, this would have caused a reduction of only 0.240 N in the total weight of the structure, being only 0.06% of the total weight of the structure. Such a reduction is below even the very strict convergence criterion of the optimization procedure and it is by no means practical from an engineering point of view, and, therefore, it seems unimportant that the optimizer does not pursue this reduction. It should be noticed that this comment applies also to small cross-sectional changes in elements 16 and 17, which are short elements.

B. Case II

The changes of the weight at the end of each model are given in Table 1. One new feature which appears in the Table

Table 2 Details of the optimized 17-bar structure[a]

	Case I Perfect structure	Case II Local imperfection		Case III System imperfection		Case IV Local and system imperfections		Case V Using safety factor	
Element	Cross-sectional area, cm^2	Cross-sectional area, cm^2	Change, %	Cross-sectional area, cm^2	Change, %	Cross-sectional area, cm^2	Change, %	Cross-sectional area, cm^2	Change (compared to Case IV), %
1	9.181	10.574	15	11.948	30	13.219	44	17.613	35
3	7.348	8.781	19	10.148	38	10.990	50	16.297	43
5	7.516	8.509	13	8.974	19	10.439	39	11.606	14
7	7.581	8.426	11	8.677	14	10.161	34	9.348	− 8
9	7.271	7.419	2	7.426	2	7.587	4	7.884	5
11	7.174	7.497	4	7.245	1	7.058	− 2	8.619	22
13	7.239	7.503	4	7.239	0	6.865	− 5	9.148	34
15	1.632	1.329	−19	1.452	− 6	1.090	−33	3.316	−27
16	0.858	0.877	2	1.535	79	1.406	64	2.865	9
17	1.219	1.194	− 2	1.548	27	0.819	−33	3.497	185
Total weight	372.8 N	410.2 N	10	431.1 N	16	462.5 N	24	564.8 N	22

[a] Note that the structure is symmetric.

is the case where convergence cannot be achieved in analyzing the resultant design of a certain optimization procedure. Such a phenomenon can be expected in nonlinear behavior, when the structure is close to collapse (which is so in the present case) and this collapse is not predicted accurately enough by the approximate model. Therefore, at the end of the optimization stage while the approximate analysis does not predict the collapse, the structure in fact is not capable of carrying the load and, therefore, the analysis does not converge.

The method of coping with such a situation is as follows: If the analysis does not converge after a certain number of iterations (15 in the present case) then all the design variables are increased by a certain amount (1% in this case), and the optimization procedure is continued in a more refined manner.

The optimum design of case II was taken at the end of the seventh model. The most important active constraint in the present case is the system buckling constraint that influences the final design more than any other constraint. The stress constraints of elements 1, 2, 7, and 8 are also active and they determine the cross-sectional areas of these elements. The details of the optimum design are given in Table 2 with the percentage of change compared to case I. One can see that the tendency in this case is to increase the flexural stiffness of the structure as a whole in order to cope with the system buckling constraint. The total weight is 410.2 N which is an increase of 10% compared to case I.

C. Case III

This is the case with system imperfection. As can be seen from Table 1 12 models are required for convergence, but from a practical point of view an optimum design is obtained early on (a convergence criterion of 0.001 is very strict). The system imperfection causes the displacement constraint, associated with displacement of node 1 in the X direction, to become the most important constraint, influencing the design more than the other constraints. In order to cope with this constraint, the tendency to increase the flexural stiffness of the structure as a whole is increased (compared to case II) and elements 1-8 are strengthened according to this tendency. The dimensions of elements 9-14 are determined mainly by the local buckling constraints of elements 9, 11, and 13. The total weight of the structure is 431.1 N which is an increase of 16% compared to the optimum of case I.

D. Case IV

This case incorporates both local and system imperfections. The optimum design in this case is given in Table 2. The tendency to increase the overall flexural stiffness of the structure is stronger in this case compared to all the other cases. The increase in the cross-sectional areas of elements 1-8 lies between 34-50% compared to case I. In the other elements the tendency is mixed and while the cross-sectional areas of a few elements are increased, others are decreased. A dominant constraint in this case is again the displacement constraint associated with the displacement in the X direction of node 1. Other active constraints are the stress constraints of elements 2, 6, 8, and 17. In elements 4 and 9 the stress is only 1% below the allowable value. The total weight of the structure is 462.46 N which is an increase of 24% compared to the optimum of case I.

E. Case V

As was pointed out before, it has been well known for a long time that optimum structures are sensitive to imperfections. The present report presents one way to cope with this problem. People have tried to cope with the same problem in other ways. In what follows, another method to introduce the influence of imperfections into the design is presented and compared with the results according to the present analysis.

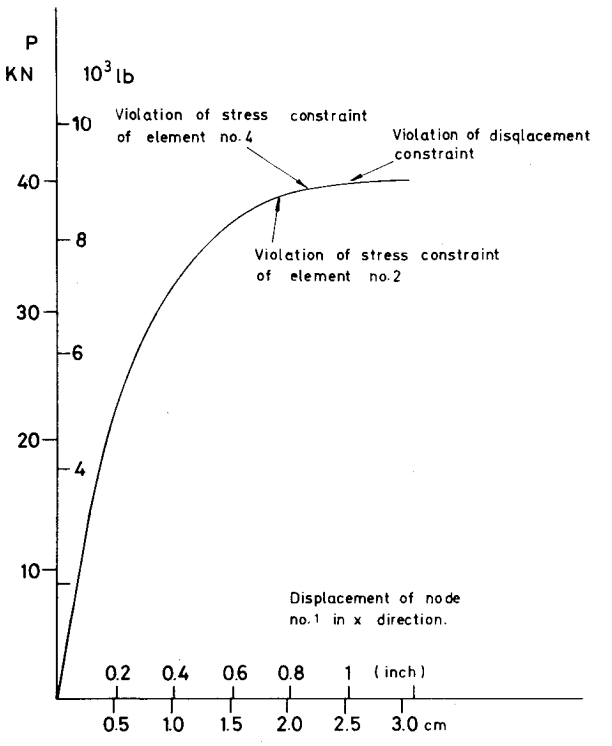

Fig. 3 Behavior of the optimized structure of case I when local and system imperfections have been added.

The optimum design of the perfect structure as presented in Table 2 (case I) is adopted, and both local and system imperfections are introduced into this design. Then the behavior of this structure is investigated. The results of this behavior are shown in Fig. 3. It is evident that due to the introduction of the imperfections the structure is not capable of carrying the original load of 75616 N. At a load of 38920 N a violation of the stress constraint of element 2 occurs and later on, as the load is increased, other constraints are violated (see Fig. 3). The structure practically collapses at a load of 40032 N. Therefore, one can conclude that due to the presence of the imperfections the load carrying capacity of the optimized structure is reduced by a factor of 0.515 (38920/75616). Therefore, if we are applying the optimization procedure to a perfect structure, the influence of the imperfections can be taken into account by applying a compressive load of 146827 N to the structure (75616/0.515), instead of the original 75616 N. (Optimization of such a structure is presented in Tables 1 and 2 as case V.)

The initial design of this case was as follows: The cross-sectional areas of elements 1-8 were 25.80 cm^2 while the cross-sectional areas of elements 9-17 were 19.35 cm^2. The total weight of the initial design was 1142.6 N. The weight of the optimum design at the end of each model is given in Table 1. As one can see, the total weight of the optimum design is 564.81 N. In Table 2 the cross-sectional areas of this optimum design are given and the percentage of change between this case and case IV is also included. One should note that the optimum of case V is considerably different from that of case IV. In case V the system buckling constraint is the most important one and its requirement to increase the flexural stiffness of the structure determines the cross-sectional areas of elements 1-6. The cross-sectional areas of elements 7-14 are mainly determined by local buckling constraints. The weight of the optimum design in case V is 22% higher than the weight of the optimum design of case IV. It should be emphasized that not only is the optimum of case V much heavier, but the fact is that, although there is certain logic in the approach, there is not any confidence that the design is really feasible.

Based on the example of case V one can conclude that the technique to optimize imperfect structures, which has been

presented in this report is better than other techniques that are based on applying certain safety factors. The advantages of the present approach lie in the fact that the optimum that is obtained turns out to be much lighter and it is surely feasible, while the results of the other techniques can also be infeasible.

At the end it may be useful to give typical computer run times. These results were obtained using an IBM370/168 computer. Cases I, II, III, IV, and V required 77, 123, 88, 149, and 115 s, respectively. Since these run times include compilation, and remembering the very strict convergences criteria, it is expected that practical run times will be much shorter.

V. Conclusions

It was shown that by using an approximate analysis to describe the highly nonlinear behavior of imperfect truss structure, one can achieve an optimum design by performing only 10-15 complete analyses. Thus by applying approximate analysis during the optimization procedure one obtains an efficient tool for optimization.

The presence of imperfections influences the design considerably. In the example presented an increase of 24% in the total weight of the optimum structure due to the presence of local and system imperfections was found, compared to the perfect structure. Moreover, it should be noted that the presence of imperfections does not cause a specific proportional increase of all elements. The influence of the imperfections differs from one element to the other. In fact, due to the presence of the imperfections the nature of the design is changed and, while certain constraints become active, others, which are active during the optimization of the perfect structure, cease to be active.

Another way to cope with the problem of the imperfections' sensitivity of optimum design, is to introduce certain safety factors that will take the imperfection presence into account. Based on the numerical example of this paper it can be concluded that not only is there no confidence that the optimum design is feasible according to the other technique, but the weight of that design may be higher (22% in the present case) than the weight of optimum design according to the technique presented in this paper, which takes into account the same imperfections.

Acknowledgments

The research described in this report was supported by AFOSR Grant No. 74-2460A. The authors wish to express their gratitude to A. Sheskin for his help with the programming and D. Rosen for preparation of the figures. The first author would also like to acknowledge the financial assistance provided by the Lady Davis Foundation, Jerusalem, Israel, for partial funding of some of the expenses associated with his post-doctoral appointment at UCLA. Most of the research reported in this paper was done during his stay at UCLA.

References

[1] Koiter, W. T. and Skaloud, M., "Interventions, Comportement Postcritiques des Plaques Utilisees en Construction Metallique," *Colloque International tenu a l'Universite de Liege, Memoires de la Societe Royale des Sciences de Liege,* 5me serie, tome VIII, fascicule 5, 1962, pp. 64-68, 103, 104.

[2] Thompson, J. M. T. and Lewis, G. M., "On the Optimum Design of Thin Walled Compression Members," *Journal of the Mechanics and Physics of Solids,* Vol. 20, 1972, pp. 101-109.

[3] Thompson, J. M. T., "Optimization as a Generator of Structural Instability," *International Journal of Mechanical Sciences,* Vol. 14, 1972, pp. 627-629.

[4] Thompson, J. M. T. and Supple, W. J., "Erosions of Optimum Designs by Compound Branching Phenomena," *Journal of the Mechanics and Physics of Solids,* Vol. 21, 1973, pp. 135-144.

[5] Thompson, J. M. T. and Hunt, G. W., *A General Theory of Elastic Stability,* John Wiley & Sons, London, 1973.

[6] Cox, H. L., "Comment," *International Journal of Mechanical Sciences,* Vol. 15, 1973, pp. 855-857.

[7] Crawford, R. F. and Hedgepeth, J. M., "Effects of Initial Waviness on the Strength and Design of Built-Up Structures," *AIAA Journal,* Vol. 13, 1975, pp. 672-675.

[8] Rosen, A. and Schmit, L. A., "Design Oriented Analysis of Imperfect Truss Structures - Part I - Accurate Analysis," *International Journal for Numerical Methods in Engineering,* Vol. 14, 1979, pp. 1309-1321.

[9] Rosen, A. and Schmit, L. A., "Design Oriented Analysis of Imperfect Truss Structures - Part II - Approximate Analysis," *International Journal for Numerical Methods in Engineering,* Vol. 15, 1980, pp. 483-494.

[10] Schmit, L. A. and Miura, H., "Approximation Concepts for Efficient Structural Synthesis," NASA CR-2552, March 1976.

[11] Haftka, R. T. and Starnes, J. H., "Application of a Quadratic Extended Interior Penalty Function for Structural Optimization," *AIAA Journal,* Vol. 14, 1976, pp. 718-724.